NASA TECHNICAL MEMORANDUM NASA TM-75795

TRANSONIC SMALL DISTURBANCES EQUATION APPLIED TO THE SOLUTION OF TWO-DIMENSIONAL NONSTEADY FLOWS

M. Couston, J.J. Angélini, P. Mulak

Translation of "Application de l'Equation des Petites Perturbations Transsoniques aux Calculs d'Ecoulements Bidimensionnels Instationnaires," La Recherche Aérospatiale, 1979, No. 5 (Sep - Oct) p. 325 - 340.

NATIONAL AERONAUTICS AND SPACE ADMINISTRATION
WASHINGTON, D.C. APRIL 1980

STANDARD TITLE PAGE

1. Report No. NASA TM- 75795	2. Government Accession No.	3. Recipient's Catalog No.
4. Title and Subtitle TRANSONIC SMALL DISTURBANCES EQUATION APPLIED TO THE SOLUTION OF TWO-DIMENSIONAL NONSTEADY FLOWS		5. Report Date April 1980 6. Performing Organization Code
7. Author(s) *M. Couston, **J.J. Angélini, *P. Mulak * Ingénieurs de Recherche à l'O.N.E.R.A. ** Adjoint au Directeur Scientifique pour l'Aéroélasticité à l'O.N.E.R.A.		8. Performing Organization Report No. 10. Work Unit No. 11. Contract or Grant No. NASw - 3199
9. Performing Organization Name and Address Leo Kanner Associates Redwood City, California 94063		13. Type of Report and Period Covered Translation
12. Sponsoring Agency Name and Address National Aeronautics and Space Administration, Washington, D.C. 20546		14. Sponsoring Agency Code

15. Supplementary Notes

Translation of "Application de l'Equation des Petites Perturbations Transsoniques aux Calculs d'Ecoulements Bidimensionnnels Instationnaires," La Recherche Aérospatiale 1979, No. 5 (Sep - Oct), p. 325 - 340. (A80-12357)

16. Abstract

Transonic nonsteady flows are of large practical interest. Aeroelastic instability prediction, control figured vehicle techniques or rotary wings in forward flight are some examples justifying the effort undertaken at ONERA to improve knowledge of those problems. This paper is devoted to the numerical solution of these problems under the potential flow hypothesis. The use of an alternating direction implicit scheme allows the efficient resolution of the two-dimensional transonic small perturbations equation.

17. Key Words (Selected by Author(s))	18. Distribution Statement
(NASA thesaurus): Unsteady flow - Aeroelasticity - Transonic flow - Two dimensional flow - Pressure distribution.	Unclassified-Unlimited

19. Security Classif. (of this report)	20. Security Classif. (of this page)	21. No. of Pages	22. Price
Unclassified	Unclassified	36	

ANNOTATIONS

c	:chord
h	;vertical airfoil displacement
k	:reduced frequency
n	:perpendicular to the surface
t	: time
x	: x axis
y	: y axis
C_l	:coefficient of lift
C_m	:coefficient of moment at the first quarter
C_p	:coefficient of pressure
D_{xx}	:mixed operator of finite difference
L	:functional
M	:Mach number
S	:surface
T	:effect period
U	:velocity
W	:velocity of the wall
α	:angle of the wall with direction x
α	:angle
γ	:specific heat ratio
δ	:sinusoidal oscillation amplitude (degrees)
δ	:relative density
δ	:finite difference operator
ε	:small quantity
χ	:coefficient of the nonlinear term
ρ	:density
τ	:control surface rate
φ	:perturbation potential
ω	:oscillation frequency
Γ	:circulation
ϕ	:velocity potential
ϕ	:phase
ψ	:periodic time function
[o]	:degrees

Indices:

i	:unsteady
j	:x axis index
k	:y axis index
l	:lift
m	:moment or mean
n	:time index or perpendicular direction
t	:in time
y	:in direction y
x	:in direction x
Z	:lift
~	:intermediary value
δ	:control surface
*	:critical value
∞	:nonperturbed flow value

Abbreviations:

S.P.T.	Small transonic perturbations equation
A.D.I.	Alternating direction implicit scheme
B.F.	Low frequency
H.F.	High frequency
C.A.C.	Control configured vehicle (CCV) techniques

TRANSONIC SMALL DISTURBANCES EQUATION APPLIED TO THE SOLUTION OF TWO-DIMENSIONAL NONSTEADY FLOWS

M. Couston, J.J. Angélini, P. Mulak
O.N.E.R.A.

SUMMARY /325*

Transonic nonsteady flows are of large practical interest. Aeroelastic instability prediction, control configured vehicle (CCV) techniques or rotary wings in forward flight are some examples justifying the effort undertaken at ONERA, in the theoretical and experimental fields in order to improve the knowledge of these problems.

This paper is devoted to the numerical solution of these problems under the potential flow hypothesis. The use of an alternating direction implicit (ACI) scheme allows the efficient resolution of the two dimensional transonic small perturbations equation.

As a first step, numerical solutions based on the low frequency assumption are compared to results provided by the linear Doublet-Lattice-method. Then it is shown that the higher order time derivatives can be taken into account, resulting in an extension of the domain of validity of the calculations toward higher frequencies.

A second step is the comparison of nonlinear results with experiments and calculations by other methods. It shows that the present method can be used to solve complex nonsteady aerodynamic problems including the determination of the shock wave movements. The comparison with experiments is affected by viscosity effects and wind tunnel wall interferences, but shows that the unsteady boundary layer acts mainly on the modulus of the unsteady aerodynamic coefficients.

I - INTRODUCTION /326

The determination of unsteady flow characteristics is highly significant for such problems as the aeroelastic instabilities of wings, the performance of rotary wings in forward flight. Current methods

*Numbers in the margin indicate pagination in the foreign text.

of calculation applied are based on linear formulations (lifting line, Doublet-Lattice, ...); no excursion in the transonic domain is thus possible, since the shock waves produce very large nonlinearities. This seriously limits the possibilities of prediction and fully justifies the efforts undertaken at ONERA, in the theoretical and experimental fields in order to improve the understanding of unsteady transonic problems.

A possible approach to these problems is the solution of the so-called Euler conservation equations (mass, momentum and energy). This approach was selected by Magnus and Yoshihara (1, 2) or Lerat and Sides (3, 4). The results are satisfactory, but the calculation time is excessive for practical applications. These methods are based on the hyperbolic characteristic of unsteady equations and use an explicit method of the problem. The explicit method of solution requires the consideration of the Courant-Friedrichs-Lewy stability criterion (C.F.L.). This criterion is translated by a time quantification, with an extremely small time interval, compared to that required to describe the unsteady effect correctly, which explains the long calculation time. An interesting way to alleviate this problem is to construct an implicit scheme. Even though the Euler equations are not suited for the implicit calculation, Beam and Warming (5) & Steger (6) have studied this possibility, although the improvements made are still modest.

More recently, an alternating direction implicit scheme (A.D.I.) has been suggested by Ballhaus et al. (7, 8). This method has been applied to the small transonic perturbations equation under the assumption of small frequencies. The scheme used is similar to that developed by Douglas and Gunn (9) to solve the heat equation. A linear stability analysis demonstrates that this technique is unconditionally stable (7). The calculation time is thus more more favorable, particularly at low frequencies where it is 100:1 faster than the explicit method of the Euler equations.

The implicit, small perturbations approach is selected in this paper. This choice is based mainly on the concern to save calculation

time. It is in fact necessary to investigate applications composed of numerous parametric scannings (Mach, reduced frequency, angle, control surface deflection...), or to consider a subsequent three-dimensional development with reasonable operating costs. Special attention is focused on the small perturbations formulation and the related boundary conditions. The possibility of easing the low frequency constraints by introducing higher order time derivatives is also demonstrated. The calculation of flows around various airfoils shows that it is possible to obtain valuable results for relatively thick airfoils. The importance of wall and viscous effects is also clearly brought to light during the comparisons of calculations and experiments.

II - DERIVATION OF THE SMALL PERTURBATIONS EQUATION

II.1 - SMALL FORMULATION AND FUNCTIONAL APPROACH

The traditional Duderley-von Karman form of the small transonic perturbations equation is the subject of some criticism. Accordingly, empirical or semiempirical laws have been introduced to "adjust" the results; refer to Ballhaus (10) or Krupp (11). Based on a formulation preserving the conservation equation characteristic, a modified equation has been suggested for the steady case. The approach to the problem, which is presented here, makes it possible to obtain similar corrections, but more reliable ones. Furthermore, this approach has been expanded further than that in reference (12), as it establishes a direct relationship between the pressure coefficient, the conservation equation and the boundary conditions. /327

In the case of potential flows, the Euler equations are reduced to the equation of continuity:

$$k\frac{\partial \rho}{\partial t} + \operatorname{div}\left[\rho \operatorname{grad}^2 \phi\right] = 0 \qquad (1)$$

where ρ is a function of ϕ provided by the Bernouilli relationship:

$$k\frac{\partial \varphi}{\partial t} + \frac{1}{2}\left[\text{grad}^2(\varphi) - 1\right] + \frac{\rho^{\gamma-1} - 1}{(\gamma-1)M_\infty^2} = 0 \qquad (2)$$

where the magnitudes characterizing the flow, space and time ρ, φ, x, y, t respectively, are normalized by $\rho_\infty, cU_\infty, c, c$ and w^{-1}, where parameter k stands for the reduced frequency $(k = \omega c / U_\infty)$.

Related to the boundary condition (3), equations (1) and (2) present the problem of unsteady flows at velocity potential,

$$\frac{\partial \varphi}{\partial n} = W_n(X, Y, t) \qquad (3)$$

where W_n is the standard velocity of the airfoil.

If we consider only the periodic flow solution in time and with a small amplitude and if the continuity equation is expressed in the weak form, for an arbitrary and periodic function ψ, by considering that $\rho(\varphi)$ is given by the Bernouilli relationship, the problem becomes:

$$\begin{aligned}
&\int\int\int \psi\left[k\frac{\partial \rho}{\partial t} + \text{div}\,(\rho\,\text{grad}(\varphi))\right] dx\,dy\,dt - \\
&\qquad - \int_0^T dt \oint_* \rho\psi\left[\frac{\partial \varphi}{\partial n} - W_n\right] ds - \\
&- \int\int \psi(x, y, 0)\left[\rho(x, y, T) - \rho(x, y, 0)\right] dx\,dy = 0.
\end{aligned} \qquad (4)$$

*airfoil

Regardless of ψ, the solution of the problem now contains both the continuity equation (first term of equation (4)) and the space and time boundary conditions (respectively by the second and third terms of (4)). Let us point out that the continuity equation represents a divergence in the time space. To convert (5) and apply the Green-Ostrogradsky theorem, we replace (4) by (6).

$$\text{div}\,\vec{A}\varphi = \text{div}(\varphi\vec{A}) - \vec{A}\cdot\text{grad}\,\varphi$$

$$\int\int\int\int \varphi\left[k\frac{\partial}{\partial t}\left(\frac{\partial\varphi}{\partial x}\frac{\partial\psi}{\partial x}+\frac{\partial\varphi}{\partial y}\frac{\partial\psi}{\partial y}\right)\right]dx\,dy\,dt = \tag{5}$$

$$= \int_0^T dt \oint_{*} \varphi\frac{\partial\psi}{\partial n}W_n\,dS \tag{6}$$

*airfoil

The first member of (6) represents the Gateaux differential (8) of a functional (9) which is connected in the steady state to the Bateman variational principle (12). The problem now becomes:

$$\delta L(\phi) = \int_0^T dt \oint_{*} \varphi\frac{\partial\psi}{\partial n}W_n\,dS = 0 \tag{7}$$

*airfoil

where the Gateaux derivative $\delta L(\phi)$ is defined as follows:

$$\delta L(\phi) = \left[\frac{L(\phi+\lambda\varphi) - L(\phi-\lambda\varphi)}{2\lambda}\right]_{\lambda=0}. \tag{8}$$

Since the functional $L(\phi)$ is the integral on the entire space-time domain of the pressure coefficient

$$L(\phi) = \int\int\int C_p(\phi)\,dx\,dy\,dt = \int\int\int \frac{\rho(\phi)^\gamma - 1}{\gamma M_\infty^2}\,dx\,dy\,d \tag{9}$$

with $\rho^\gamma(\phi)$ provided by the relationship (2).

We thus see that the problem presented by equation (7) is in the weak form equivalent to the initial problem, but the continuity equation and the boundary conditions are regrouped. Accordingly, it is possible to relate a continuity equation and modified boundary conditions to any approximation of the functional (hence of the pressure coefficient); this procedure will be followed in the next paragraph.

II.2 - APPROXIMATION IN THE DIRECTION OF SMALL PERTURBATIONS

As long as we focus on small perturbations of a uniform flow, it is practical to introduce the perturbation potential φ. The Bernouilli relationship therefore makes it possible to express ρ^γ by using φ:

$$\left(1 - (\gamma - 1)M_r^2 \left[k\frac{\partial \varphi}{\partial t} + \frac{\partial \varphi}{\partial x} + \frac{1}{2}\,\mathrm{grad}^2 \varphi\right]\right)^{\frac{1}{\gamma-1}}. \tag{10}$$

We thus have the following expression:

$$\rho^{\gamma-1} = (1+\varepsilon)^{\gamma-1} \tag{11a}$$

is a small quantity. A series expansion gives:

$$\rho^{\gamma-1} = 1 + (\gamma-1)\varepsilon + \frac{1}{2}(\gamma-1)^2\varepsilon^2 + \ldots \tag{11b}$$

We can thus truncate this series by considering the respective order of all derivatives by a similar approach, such as the Miles approach (14). This is even easier here since we have only the first derivatives. Reference (15) would consider the low frequency case, i.e.:

$$k = \omega^2 \cdot (1 - M_r^2) \sim \varepsilon \ll 1 \tag{12}$$

where ε is the perturbation parameter. In order to extend the expansion validity toward higher frequencies, we assume here:

$$k^2 = \omega^2 \cdot (1 - M_r^2) \sim \varepsilon \ll 1. \tag{13}$$

By truncating the expansion of ρ^{γ} with the order ε^3 the functional is expressed as follows:

$$\begin{aligned} L(\varphi) = \int\int\int \Bigg[& \frac{\partial \varphi}{\partial x} + k\frac{\partial \varphi}{\partial t} - k M_r^2 \frac{\partial \varphi}{\partial x}\frac{\partial \varphi}{\partial t} + \\ & + \frac{1 - M_r^2}{2}\left(\frac{\partial \varphi}{\partial x}\right)^2 + \frac{1}{2}\left(\frac{\partial \varphi}{\partial y}\right)^2 - \\ & - \frac{1}{6}\left\{(\gamma+1)M_r^2 + 3(1 - M_r^2)\right\} M_r^2 \left(\frac{\partial \varphi}{\partial x}\right)^3 - \\ & - \frac{k^2 M_r^2}{2}\left(\frac{\partial \varphi}{\partial t}\right)^2 \Bigg] dx\, dy\, dt \end{aligned} \tag{14}$$

where the quantity between the brackets represents the pressure coefficient approximated in the direction of the small transonic perturbations. The last term of this quantity is that which is produced when proceeding from the low frequency approximation (12) to that of the high frequencies.(13). Based on the approximation of the functional, it is now possible to define an equation and the related boundary conditions. /328

II.3 - SMALL UNSTEADY TRANSONIC PERTURBATIONS EQUATION

From the weak formulation of the problem and the functional approach, we have shown in paragraph II.1 that there was an equivalence between the initial problem (continuity equation, plus boundary condition) and the equation (7). By evaluating the Gateaux derivative from the approached functional (14), it is possible to reconstruct an approached continuity equation:

$$k^2 M_r^2 \frac{\partial^2 \varphi}{\partial t^2} + 2k M_r^2 \frac{\partial^2 \varphi}{\partial x \partial t} = \left[(1 - M_r^2) - \lambda \frac{\partial \varphi}{\partial x} \right] \frac{\partial^2 \varphi}{\partial x^2} + \frac{\partial^2 \varphi}{\partial y^2} \tag{15}$$

with:

$$\lambda = \left[(\gamma + 1) M_r^2 + 3 (1 - M_r^2) \right] M_r^2 . \tag{16}$$

The main difference between equation (15) and the traditional equation of small perturbations lies in the value of coefficient λ defined in (16). In the traditional form of the small perturbations, Miles (14) finds for λ the value (17) which corresponds to the traditional form (called the Guderley-von Karman formula in the steady case). Krupp (11) and Ballhaus (10) correct this equation by using respectively (18) or (19). The value of m corresponding to (19) is a function of the shock intensity, values smaller than m = 1.75 are considered in (10).

Miles [14], Krupp [11], Ballhaus [10]: $\lambda = (\gamma + 1) M_r^m$

$m = 2$ (17)

$m = 1{,}75$ (18)

$m = f$ shock (19)

In order to bring to light the importance of , let us point out that the "critical velocity" , which reduces the coefficient of the second derivative to zero in x, equation (15), is a direct function of . This critical velocity, which passes equation (15) from subsonic to supersonic, is presented in figure 1 for different assumptions on . It may be noted that the traditional formula (17) is corrected, which goes in the same direction as equation (18), but without using empirical considerations. Moreover, form (16) is identical to that of reference (12).

For low frequencies (12), the first term of equation (15) disappears and the equation used by Ballhaus (7,8) or the author (15) is obtained. Equation (15) reestablishes the possibility of the double wave system, recessive and progressive, which degenerates at low frequencies (12) into a single recessive wave.

II.4 - BOUNDARY CONDITION ON THE AIRFOIL

As we have already shown from the approximated functional (14) it is possible to obtain an approached continuity equation in the direction of small perturbations (15), but at the same time we are defining the boundary condition which must be expressed on the airfoil. This boundary condition related to the equation is:

$$\frac{\partial \varphi}{\partial y} = \frac{\partial h}{\partial x}\left[1 + (1 - M_\infty^2)\frac{\partial \varphi}{\partial x} - \frac{\gamma+1}{2}\left(\frac{\partial \varphi}{\partial x}\right)^2 - kM_\infty^2 \frac{\partial \varphi}{\partial t}\right] + k\frac{\partial h}{\partial t}\left[1 - M_\infty^2 \frac{\partial \varphi}{\partial x} - kM_\infty^2 \frac{\partial \varphi}{\partial t}\right]. \tag{20}$$

We must compare it to the traditional formula, reference (14), which is:

$$\frac{\partial \varphi}{\partial y} = \frac{\partial h}{\partial x} + k\frac{\partial h}{\partial t} \tag{21}$$

where h(x,t) is the function describing the geometry of the airfoil.

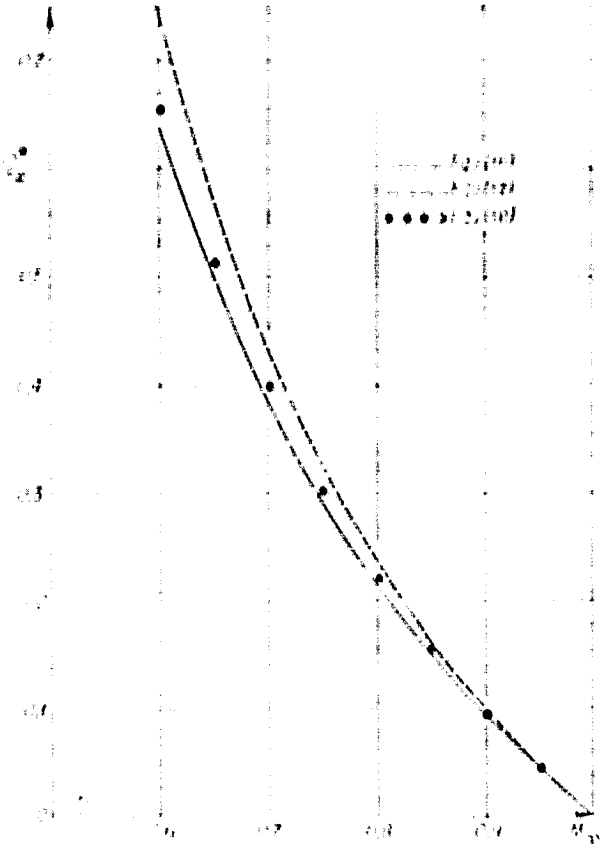

Fig. 1 - Critical Velocity

It may be emphasized that the additional terms introduced by the present approach are as small as the perturbations, but must not be omitted if there is compatibility between the equation of the small transonic perturbations (15) and the boundary conditions. Later on, we shall see that the additional terms in (20) make it easier to predict the leading edge which is always a critical place for solving the small transonic perturbations equation.

II.5 - SLIP-STREAM POTENTIAL SHIFT

In the solution of the velocity potential problem, we must define the potential displacement (or circulation) through the slip-stream which develops at the trailing edge. For the small perturbations, the slip-stream equation is expressed on a horizontal cut and must represent the pressure coefficient continuity. Accordingly, for the small transonic perturbations equation at low frequencies, we generally consider that the pressure equation is given by (22a); hence, the potential displacement must satisfy 22b. This means that the circulation Γ is not a function of the x axis, but only of time (22b). /329

$$\frac{C_p}{2} + \frac{\partial \Gamma}{\partial x} = 0 \qquad (22a)$$

$$\frac{\partial \Gamma}{\partial x} = 0; \quad \Gamma = F(t). \qquad (22b)$$

This assumption, which is selected by Ballhaus (8), for example, may be considered as too narrow to the extent that it is the same as assuming that the circulation moves at an infinite velocity. By recalling that the functional (14) represents the integral of the pressure coefficient, the compatibility between the equation and the slip-stream must be ensured by assuming the continuity of this approached value C_p. The equation thus obtained is quite a bit more complex and lends itself poorly to the subsequent numerical calculation. A partial improvement of (22) may be easily introduced, by keeping the first two terms of the of the pressure coefficient expansion, which is the same as expressing (23a). We thus obtain a hyperbolic equation on Γ (23b), which translates the circulation velocity transfor of the nonperturbed fluid (per unit for normalization).

$$\frac{C_p}{2} + k\frac{\partial \Gamma}{\partial t} + \frac{\partial \Gamma}{\partial x} = 0 \qquad (23a)$$

$$k\frac{\partial \Gamma}{\partial t} + \frac{\partial \Gamma}{\partial x} = 0; \quad \Gamma = F(x, t). \qquad (23b)$$

Hence, even though (23) is approached, it may be considered as a better approximation than (22); in fact, we know that for the full potential, the circulation moves at the local fluid velocity and not at an infinite velocity. We shall see on a few examples, in linear cases, the differences generated by using (22) or (23).

III - NUMERICAL SCHEME

The solution of the small transonic perturbations equation (15) is obtained by an extension of the alternating direction implicit scheme (A.D.I.) described by Ballhaus (7, 8). Equation (15) is split into two equations by introducing an intermediate variable Z; this makes it possible to investigate the term of the second derivative in time in a centered manner. The quantification of the two intervals n and $(n+1)\,\Delta t$ ensures the linearization of the problem:

$$kM_\infty^2 \frac{\varphi^{n+1} - \varphi^n}{\Delta t} + 2kM_\infty^2 \frac{\partial}{\partial x}\left(\frac{\varphi^{n+1} - \varphi^n}{\Delta t}\right) = \quad (24a)$$

$$\frac{\partial}{\partial x}\left[(1 - M_\infty^2)\frac{\varphi_x^{n+1}}{2} + \varphi_x^n - \frac{\lambda}{2}\varphi_{xx}^{n,n+1}\right] + \frac{\partial^2}{\partial y^2}\frac{\varphi^{n+1} + \varphi^n}{2} \quad (24b)$$

$$= \frac{Z^{n+1} + Z^n}{2} + k\frac{\varphi^{n+1} - \varphi^n}{\Delta t}.$$

The variable Z^{n+1} is therefore eliminated (24a) by using (24b); the linear and two-dimensional problem on φ^{n+1} which results is factorizedby an approximation in two steps: the first step depends on the unkown $\tilde{\varphi}$ according to x alone, the second step depends on the unkown φ^{n+1} according to y alone (since the solution is made upstream to downstream). The complete solution is presented in the following form:

-step in x

$$\frac{2kM_\infty^2}{\Delta t}\left[\frac{k}{\Delta t} + \delta_x\right](\tilde{\varphi}_{i,k} - \varphi_{i,k}^n) = D_{xx}(\tilde{\varphi}, \varphi^n) + \delta_{yy}\varphi_{i,k}^n + \frac{2kM_\infty^2}{\Delta t}Z^n \quad (25a)$$

-step in y

$$\frac{2kM_\infty^2}{\Delta t}\left[\frac{k}{\Delta t} + \delta_x\right](\varphi_{i,k}^{n+1} - \tilde{\varphi}_{i,k}) = \frac{1}{2}\delta_{yy}(\varphi_{i,k}^{n+1} - \varphi_{i,k}^n) \quad (25b)$$

-calculation step of z

$$Z_{i,k}^{n+1} + Z_{i,k}^n = \frac{2k}{\Delta t}(\varphi_{i,k}^{n+1} - \varphi_{i,k}^n) \quad (25c)$$

δ_x is the operator of the derivative decentered backward, which ensures the upstream to downstream solution.

D_{xx} is a mixed operator similar to that of Murman (16) which ensures the stability in the supersonic zones by a backward decentering and which preserves the conservation by a special investigation of the sonic points and shock points.

δ_{yy} is the operator of the second derivative centered in y

which introduces the boundary conditions of the walls in the problem.

Let us note that the main interest of scheme (25a and b) lies in the fact that it does not generate three or four diagonal matrices; the matrices may be solved effectively by factorizing them into the product of a subdiagonal and superdiagonal matrix. The step corresponding to (25c) is there only to calculate the intermediary variable which is brought to light point by point.

Figure 2 presents the type of meshing used for the calculation. The number of nodes of the domain is generally about 5,000; about 100 points are placed on the cut, which in the approximation of the small perturbations, is the line which represents the airfoil. The meshing is drawn along a geometric progression when we move back from the airfoil; the boundaries are thus far enough to avoid interfering wave reflections. The lower and higher boundary conditions correspond to the impervious and immobile walls which may be placed at an arbitrary distance. The downstream condition translates in an approached manner the presence of an isobar.

The calculation times for the numerical solution are reasonably short; hence for periodic effects, approximately 6 mn of CII-IRIS 80 per oscillation cycle (or about 1.5 mn UNIVAC 1,1110 or 15 s of CDC 7,600) must be counted.

IV - LINEAR CALCULATIONS

At the present time, unsteady aerodyanamic calculations are mainly performed by using linear methods. We may thus show the possibilities offered by this algorithm in the linear case, i.e. by doing $\lambda = 0$ in equation (15). Our results are therefore directly comparable to the Doublet-Lattice-Method developed at the ONERA from works by Albano and Rodden (17).

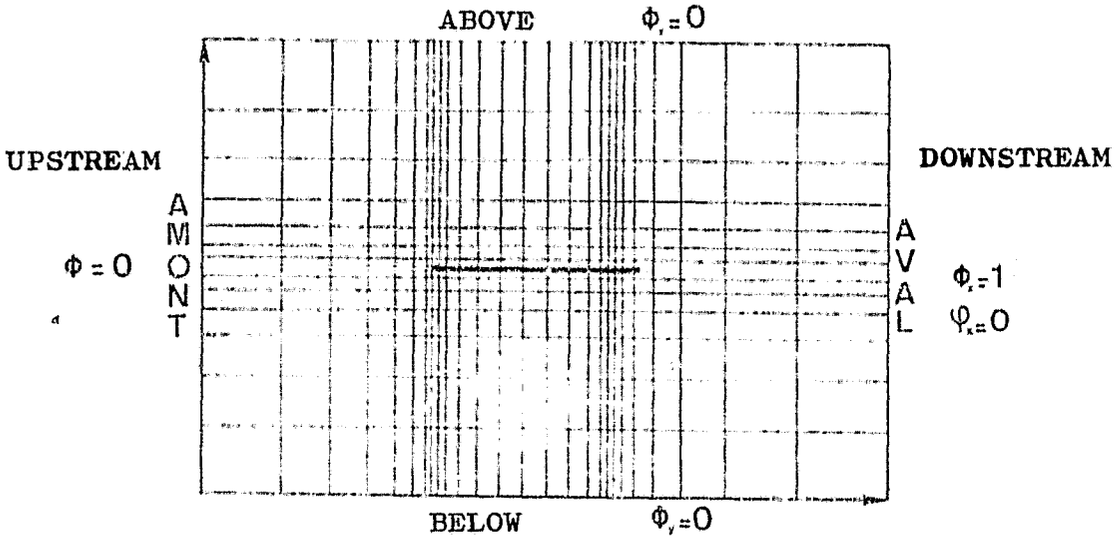

Cut (where boundary condition 15 or 15 applies)

Slip-stream — Above / Below

Fig. 2 - Calculation Domain

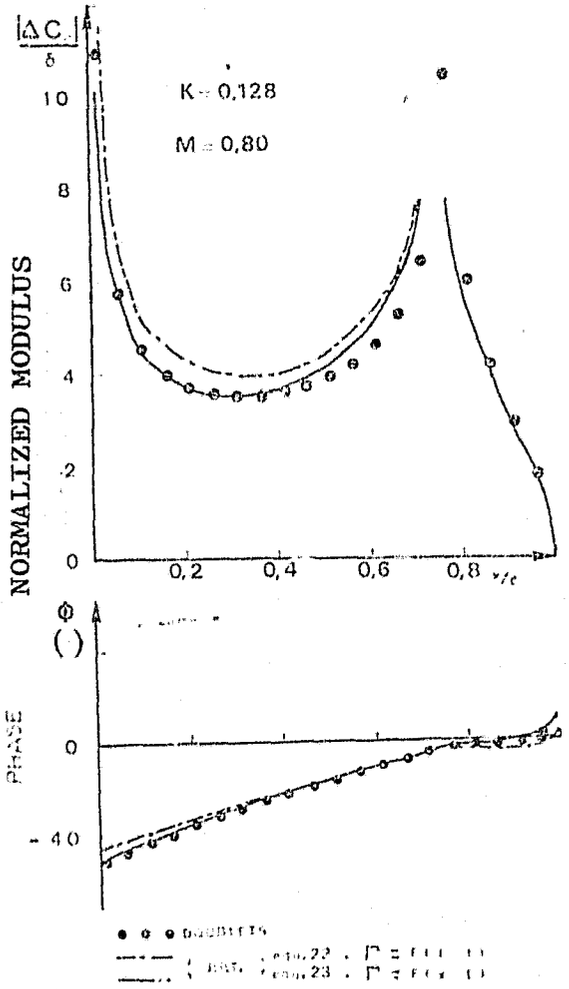

Fig. 3 - Pressure Distribution on a flat plate with oscillating control surface (linear equation)

Figures 3 to 6 are placed in the linear framework, but under the low freqencies assumption, which means that the second time derivative in equation (15) is omitted. All of these figures present the modulus and the phase of the unsteady pressure coefficient on a flat plate. Figures 3 and 4 correspond to a flap oscillation for two reduduced frequency values. The influence of the circulation on the pressure coefficient modulus may be noted, particularly for the lowest frequency (fig. 3). If the frequency is increased, the trailing edge is mainly affected. Comparison with the Doublet-Lattice-Method shows that

the prediction is better if the circulation is transported at the nonperturbed fluid velocity rather than at an infinite velocity. Hence, equation (23) will be selected. Figures 5 and 6 relate to two other motions: a pitching around a front quarter and a surging. Agreement with the Doublet-Lattice method is excellent and confirms that for frequencies of this order the term of the second derivative versus time is negligible. This is not always the case. Figure 7 presents the case of pitching of a flat plate in a wind tunnel at a reduced frequency k = 2. It is clearly obvious that the solution of the complete equation (15) (annotated here H.F.) gives a better result if the second time derivative term is omitted (annotated here B.F.). In fact, the agreement is practically perfect for the unsteady pressure coefficient phase between the H.F. equation and the Doublet-Lattice Method, whereas the assumption of B.F. introduces errors in excess of one hundred degress. As for the modulus, even though the improvement is obvious, it appears to be moderately underevaluated in comparison with the Doublets-Lattice-Method. This difference, probably introduced by the approached factorization of the equation, is a small sum as much as the reduced frequency k = 2 is characteristic of the maximum reduced frequencies found physically on the actual wings. The complete equation (15) is therefore preferred to the low frequencies equation (15) to the extent that its domain of application is wider and its calculation times are of approximately the same order.

V - NONLINEAR CALCULATIONS

/333

The nonlinear calculations will be concerned with two NACA airfoils and one supercritical airfoil developed by Aérospatiale. The first airfoil, the NACA 64 A 006, has been selected because with only 6% relative density and a small leading edge radius, it corresponds well to the small perturbations assumptions. Moreover, measurements, Tijdeman (20) and calculations, Magnus and Yoshihara (1, 2, 18, 19); Ballhaus (8, 21) or Ehlers (22), are available for comparisons to be made. The second airfoil, the NACA 0012, has a larger relative density and a less favorable leading edge; the results may be compared to those found by Lerat and Sides (3,4). The third airfoil, the RA 16 SC 1

 16 - 17

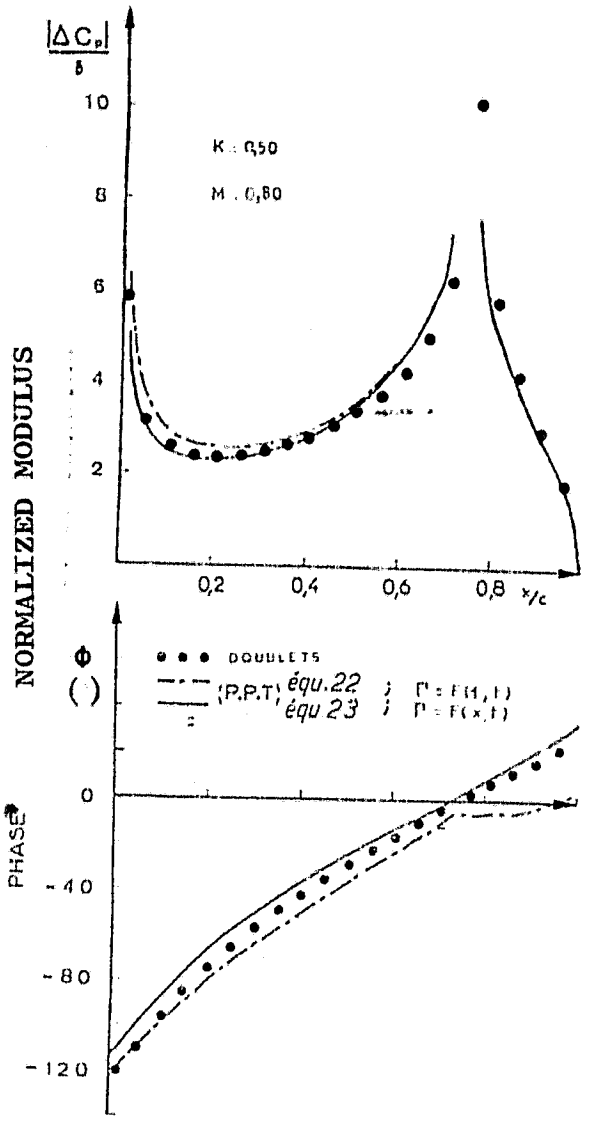

Figure 4 - Pressure distribution on a flat plate with oscillating control surface (linear equation).

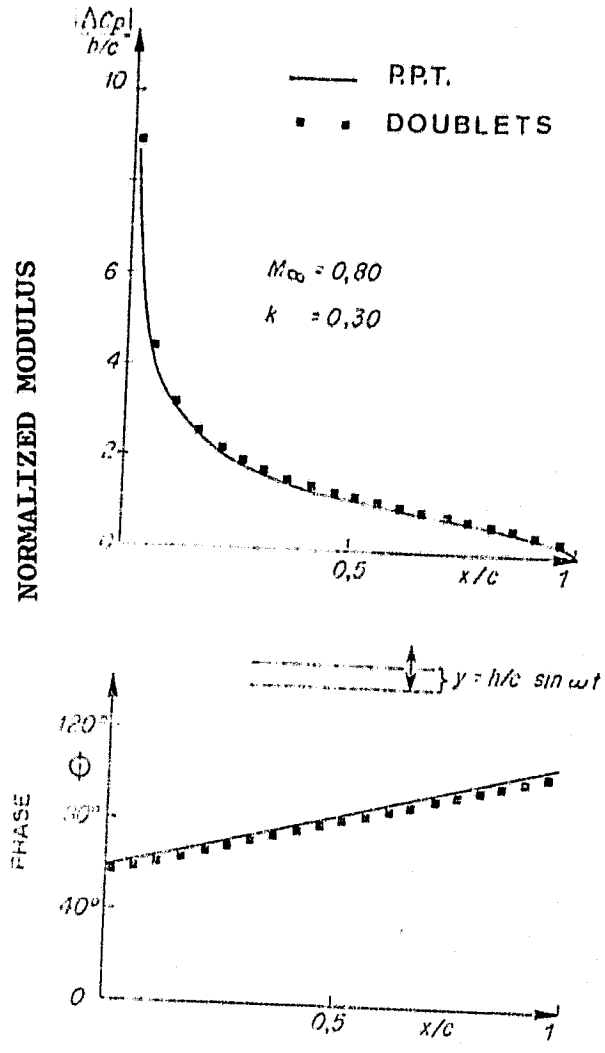

Figure 5 - Pressure distribution on a pitching flat plate.

at Aérospatiale, is a dense ($\delta \simeq 16\,\%$) but supercritical airfoil. ONERA has fitted it with an oscillating control surface and a series of two-dimensional unsteady tests in the Modane S_3 wind tunnel have provided extensive experimental information (see Grenon and Thers: 23, 24) which we may attempt to utilize.

NACA 64A006

Figure 8 presents the pressure distribution along the chord in the steady state for a Mach number $M_\infty = 0{,}875$. Comparison with Magnus and Yoshihara calculations is satisfactory. It should be pointed out that two small perturbations calculations are presented which differ by the boundary condition. These two calculations show that the behavior at the leading edge is better when equation (20) is used. In fact, the traditional form (21) shows an anomaly at the leading edge, this situation is well-known in the traditional approach, see Ballhaus (10), for example. Equation (21) thus appears to be a better choice for the investigation of the leading edge than the traditional form. It should not be concluded that all problems are eliminated in this region; in fact, small perturbations will always be wrong near a stop point.

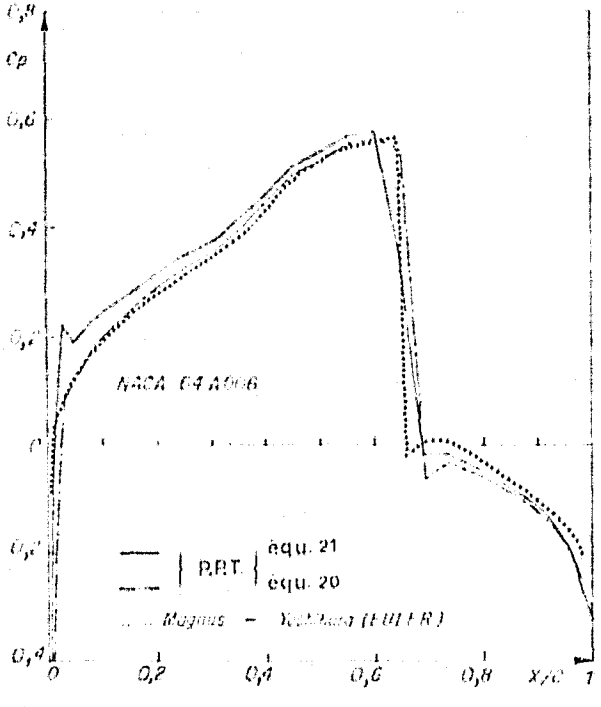

Fig. 8 - Steady Pressure

$M_\infty = 0{,}875$, $\gamma = 0°$

The unsteady case of a control surface motion in the presence of shock waves is illustrated by figure 9. The latter presents theoretical and experimental values of the modulus and of the first harmonic phase of the pressure

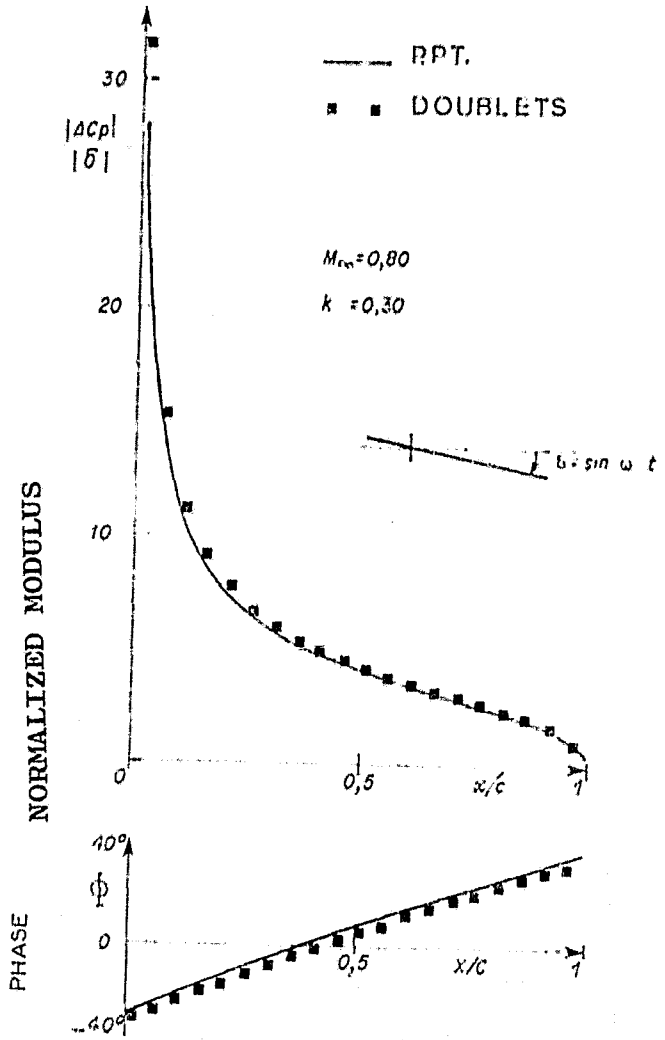

Fig. 6 - Pressure distribution on a surging flat plate

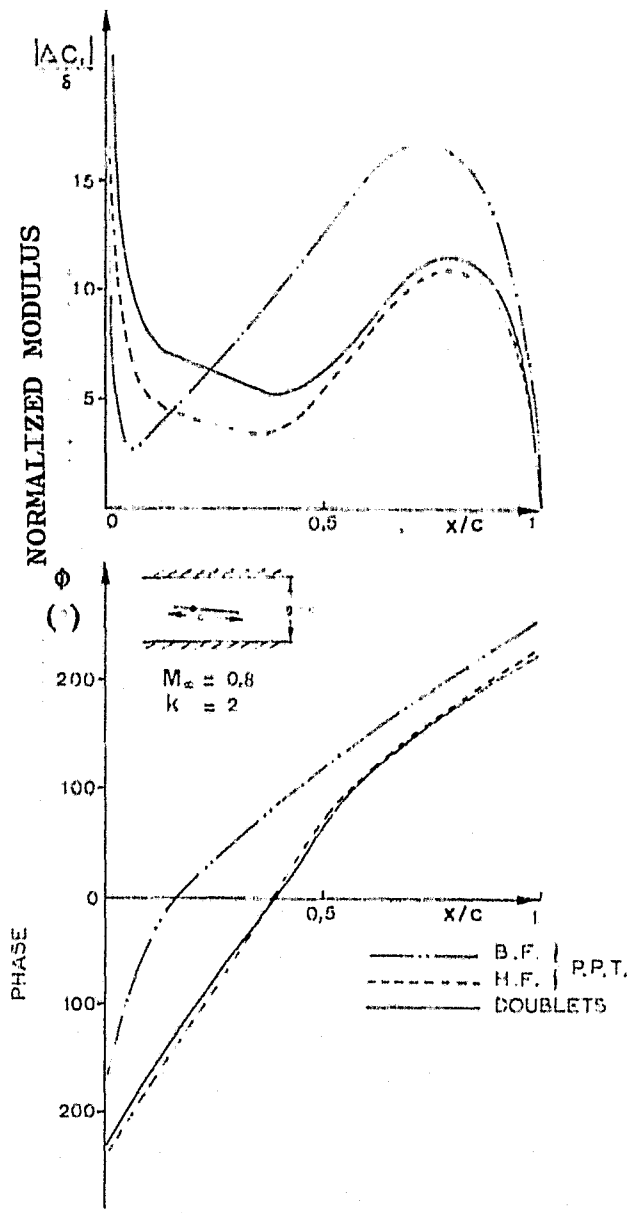

Fig. 7 - Pressure distribution on a pitching flat plate grid.

coefficient normalized by the displacement. The agreement between the results of the present method and those of Magnus (19) is relatively good; tests by Tijdeman (20), on the other hand, give quite different results. This is especially obvious in the shock region where the pressure coefficient modulus is distinctly overevaluated by the calculation. Magnus (19) suggests that we are in the presence of a viscous effect, but his semiempirical viscous corrections in the shock region have not brought a satisfactory solution to the problem. It is thus probable that it is a wind tunnel wall effect of perforated walls located at a chord and one-half from the airfoil in this case. It should be emphasized that the satisfactory comparison between the P.P.T. and the Euler equations is encouraging, especially if we consider that the calculation time here is about one hundred times shorter.

We currently know that in aeroelasticity the calculations of fluctuations make use only of linear methods: behavior in time is assumed to be harmonic. Figures 9 to 11 show why this approximation is is no longer correct in the transonic state. In fact, figure 9, the modulus of the first harmonic of the pressure coefficient has a maximum between 50 and 60% of the chord, this maximum is substantially larger than the logarithmic characteristic of the crest (75% of the chord) and is related only to the shock wave displacement. Any linear calculation will necessarily result in a distribution similar to that of figures 3 and 4 and will therfore not be representative of the problem. Figure 10 shows how the effect, which controls the shock wave displacements, is nonlinear; in fact for two oscillating amplitudes of the control surface, we obtain two quite different results for the pressure coefficient modulus (normalized by the displacement). Likewise, whereas the control surface oscillates sinusoidally, the response of the pressure coefficient is of higher order harmonics as is shown on figure 11. The transonic state thus brings into doubt the validity of the basic assumption of a fluctuation calculation, i.e. its linearity, and that of the harmonic time behavior which results. These pessimistic conclusions may be alleviated if we consider the integrated values of the unsteady aerodynamic forces (F.A.I.). For these values, the linear and harmonic behavior assumption gives acceptable results for fluctuation calculations as is shown

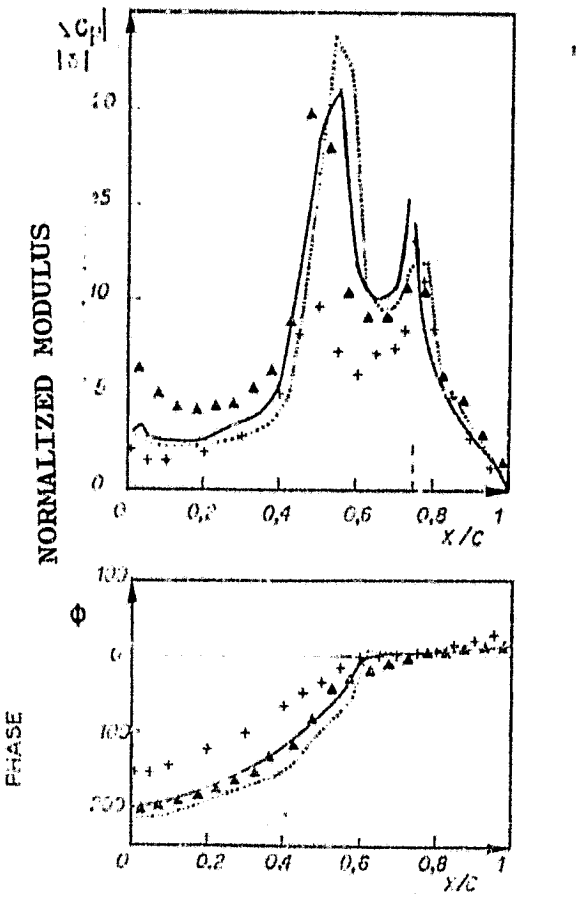

Fig. 9 - Unsteady pressure distribution on the NACA 64 A 006 airfoil with oscillating control surface (first harmonic).

P.P.T. $\delta(t) = 1° \sin(kt)$.
Magnus. $k = 0{,}358$.
Ehlers. $M_\infty = 0{,}854$.
Tijdeman.

TABLE I - Harmonicity and linearity of unsteady aerodynamic forces.

δ_t amplitude motion			0,5	1,0	1,5
$C_{z\delta}$	1st harmonic	Modul	3,51	3,51	3,50
		Phase	− 44°	− 44°	− 44°
	3rd har.	Modul	0,010	0,013	0,022
$C_{m\delta}$	1st harmonic	Modul	1,74	1,74	1,72
		Phase	− 15°	−15,5°	− 16°
	3rd har.	Modul	0,006	0,006	0,010

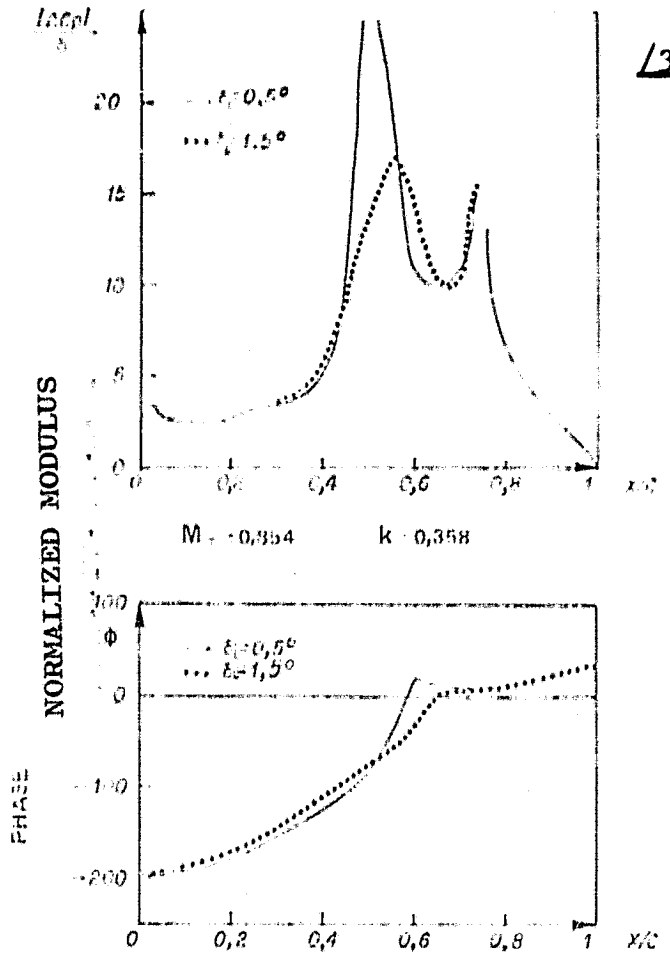

/334

Fig. 10 - Unsteady pressure distribution on the NACA 64 A 006 airfoil with oscillating control surface. (First harmonic). $M_\infty = 0{,}854$. $k = 0{,}358$.

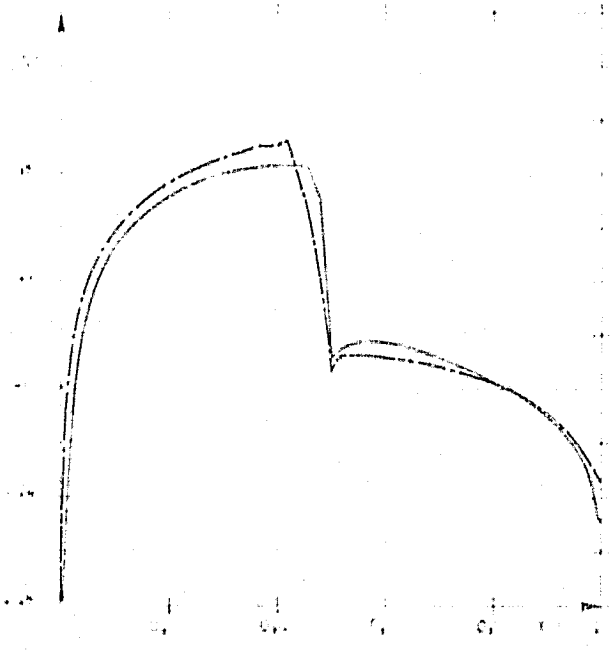

/335

Fig. 12 - Steady pressure distribution, NACA 0012 Airfoil $M_\infty = 0{,}80$. $\alpha = 0°$
P.P.T.
Euler [4].

on table I for calculations made on this airfoil.

NACA 0012

The NACA 0012 is a relatively dense airfoil (12% relative density), hence, it is profitable to compare our results with those found by the explicit solution of the Euler equations in the integral form developed at the ONERA by Lerat and Sides (4).

The steady C_p for a zero angle and $M_\infty = 0.8$, figure 12, presents a comparison of the two shock methods; the shock is approximately in the same position and the observable differences are small. Based on this steady state, we have introduced a sinusoidal control surface motion with an amplitude of 1° at a reduced frequency k = 0.5. The periodic state (on the airfoil) is established in three to four cycles, figure 13 presents the pressure distribution during the 4th cycle (eve (every 45°). It is easy to check out the good periodicity by noticing that a phase shift of 180° brings about a permutaion between the top and bottom of the airfoil. The shock wave displacement is distinct; it shows here a type A ("sindusoidal") motion described by Tijdeman (20) from wind tunnel tests. The wave shock screen effect shown on figure 12 is obvious; it may be observed that the front of the airfoil receives only very small pressure variations; these variations are /335 caused by waves passing around the supersonic sone. We are now in the presence of an essentially different subsonic effect where linear theories are applicable. Figure 14 compares the lift coefficient paths during the cycle, which were found by the two methods; if the ph phase agreement is good, the intensities differ by about 30%, a difference which is difficult to attribute to the steady field. It may be observed on figure 13, for kt = 0° or 180°, a large phase shift of the shock motion versus the control surface oscillation (which is then in the wind bed) occurs; this is the phase shift responsible for the largest portion of the unsteady lift. Accordingly, if the amplitude of the shock wave displacement is different between the two methods, the unsteady lift will be affected. Figure 15 presents the chord position (on one side of the airfoil) of the shock wave during the cycle.

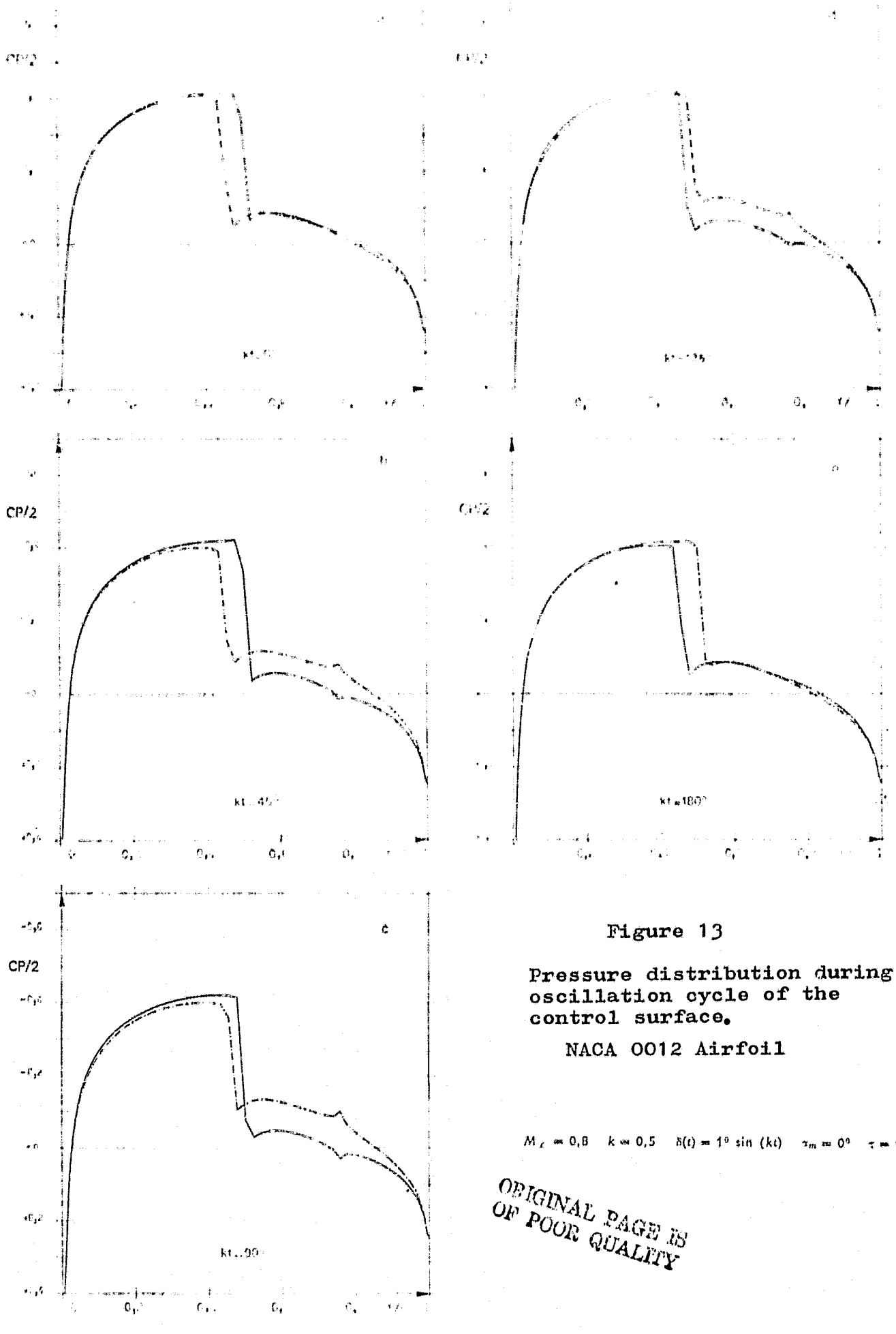

Figure 13

Pressure distribution during oscillation cycle of the control surface.

NACA 0012 Airfoil

$M_\infty = 0,8 \quad k = 0,5 \quad \delta(t) = 1° \sin(kt) \quad x_m = 0° \quad \tau = 0,25.$

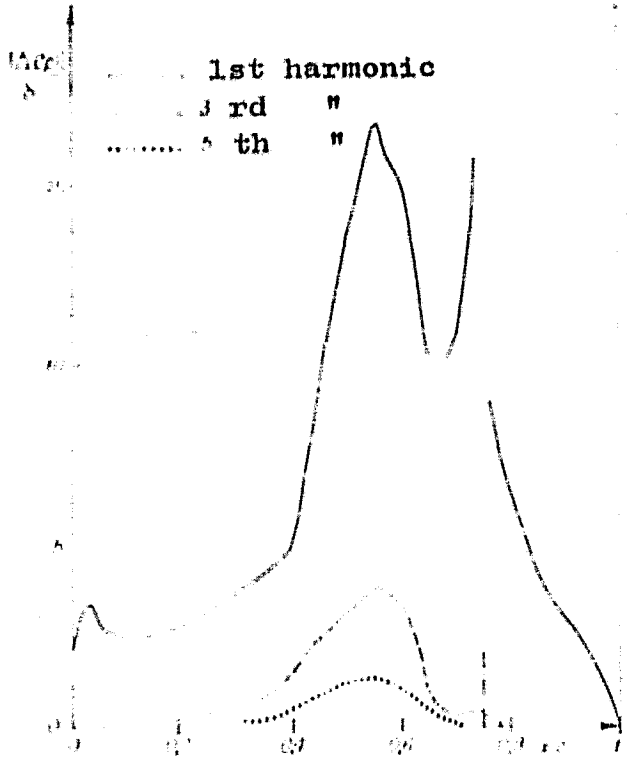

Fig. 11 - Harmonic analysis of pressure coefficient with oscillating control surface. NACA 64 A 006 Airfoil

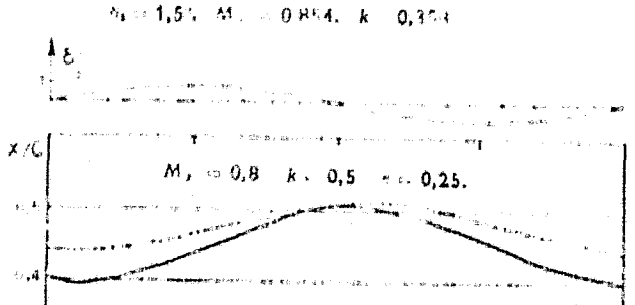

Fig. 15 - Shock displacement on lower surface. NACA 0012 Airfoil

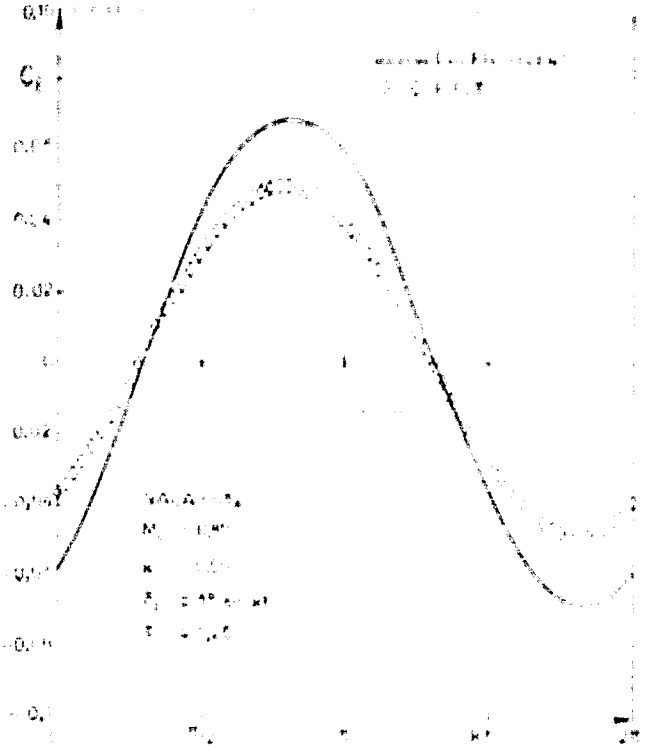

Figure 14

Evolution of the lift coefficient

/334

/337

We see that the displacement allowed by the Euler equations method has a larger amplitude which explains the difference in level in the unsteady lift evaluation. This difference still cannot be explained; we do not know if it should be attributed to the potential flow assumption, to the small perturbations approximation or to an inadequately precise numerical solution of one of the two methods. /335

The respective calculation times between the two methods are in a ratio 1 to 65 in favor of the P.P.T., which emphasizes the advantage of the method, especially if a three-dimensional extension is considered.

Aérospatiale RA 16 SC 1

Based on the preceding remarks regarding the NACA 64 A 006 airfoil, we shall keep in mind that the wall effects in the transonic state make any comparison difficult. As for the tests made on this airfoil, a few positive points should be emphasized; the level of the airflow (normalized by the airfoild chord) is higher, the critical Mach is smaller, which should assist in minimizing the blocking effects even though the airfoil is denser. Furthermore, some tests have been conducted with a guided airflow (solid walls) in order to facilitate theoretical comparisons; in fact, it is not easy to take perforated walls into account by calculation. Accordingly, we shall make our comparisons on the basis of these tests, with the calculation taking the wind tunnel walls into account. /335

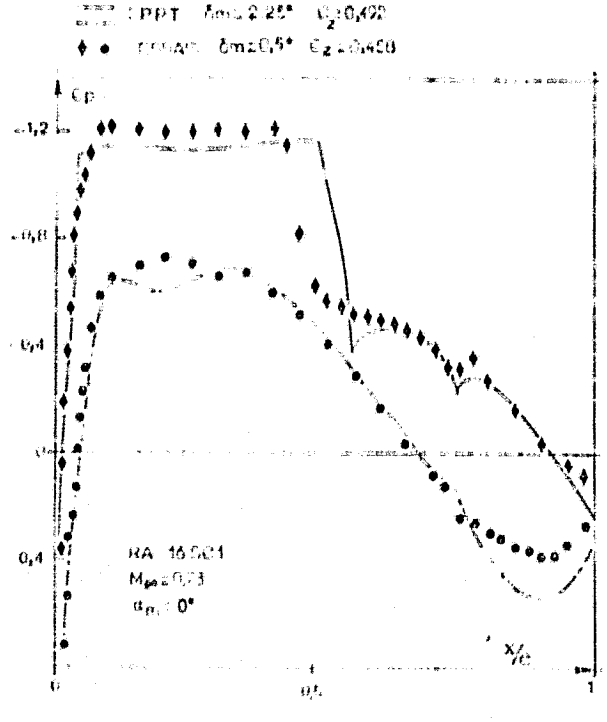

Figure 16

Cp steady. Airfoil in guided airflow

The calculated and measured steady pressure coefficients are presented in figure 16. It may be noted that the calculation and tests are different for the control surface deflection. This deflection difference makes it possible to simulate part of the viscous effects by replacing the shock in a position near the tests. If th s precaution is not taken, the shock wave is located at 85% from the chord and its intensity more than doubles. The control surface is oscillated sinusoidally around this average deflection and we obtain the periodic evolution presented on figure 17. Once again, it is the shock wave which most actively participates at the unsteady evolutions, as it is displaced on more than 10% of the

chord. It reaches its highest upstream position with a phase shift of about 90° compared to the maximum deflection of the control surface; the delay is relatively in good agreement with observations made in reference (23, 24) for this reduced frequency. Figure 18 shows the

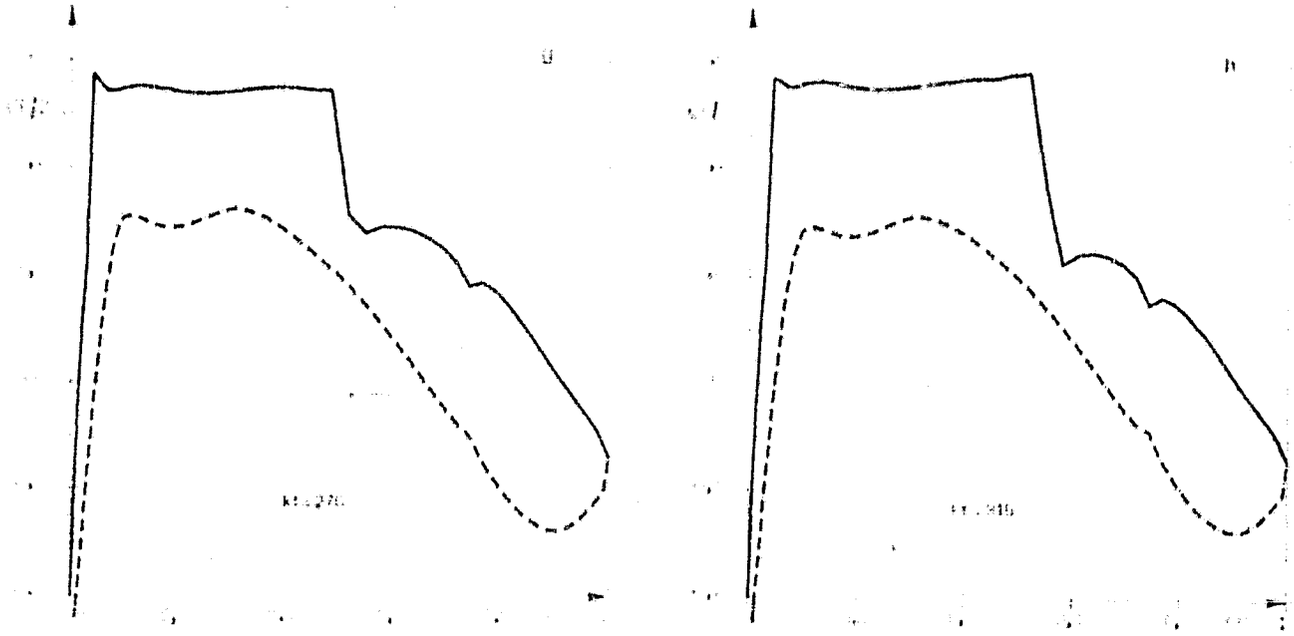

/339

Figure 17 - Pressure distribution during oscillation cycle of the control surface $M_\infty = 0,73$ $\alpha = 0°$ $\delta_m = 2,25$ $\delta(t) = 1° \sin(kt)$ $k = 0,333$ - $\varepsilon = 0,25$.

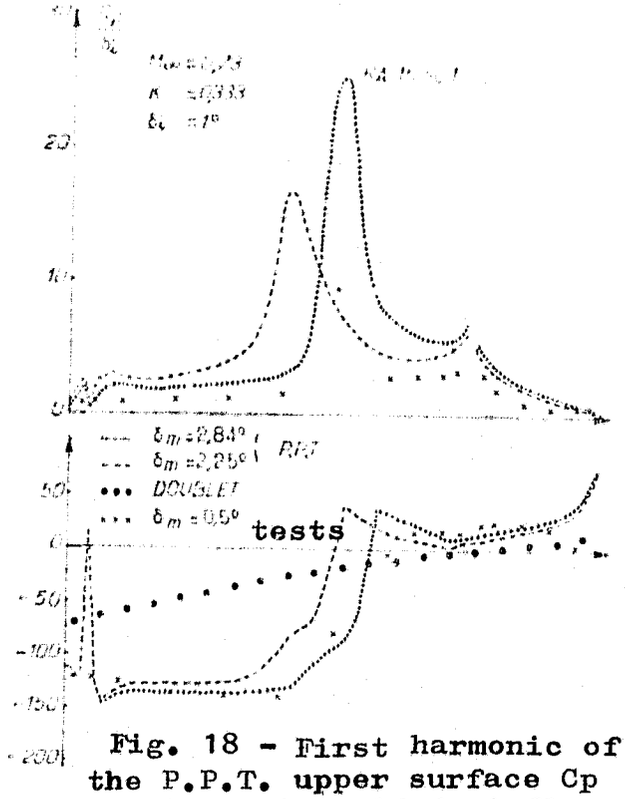

Fig. 18 - First harmonic of the P.P.T. upper surface Cp and tests in guided airflow.

first harmonic (normalized and phase modulus) of the upper surface pressure coefficient. It may be noted that if the shock is carefully (by mean deflection of the control surface) replaced in its experimental situation, we have a good agreement on the phases. It is obvious that the shock controls the effect, for if we take the Doublet-Lattice-Method into consideration, the phases are very different. It is quite obvious that the modules on figure 18 are considerably

overevaluated (more than 50% over most of the chord); it is if we had an "effective apmlitude" of control surface motion of 0.65° instead of 1°. This occurance is not characteristic of transonic flows; in fact, it may be noted in the reference (25) that even in subsonic flows for this airfoil, we have an equivalent loss of performance between the theory without boundary layer and the tests or a theory with boundary layer. Unless this loss in performance is estimated empirically or semi-empirically, it appears necessary to introduce a boundary layer idealized fluid coupling, as if it seems possible to predict the phases on the basis of steady tests and a nonviscous unsteady calculation, the modulus depends even more on viscous effects. This is what we may observe in table II where the P.P.T calculation (guided airflow) gives a correct estimate of the phases of the unsteady aerodyanmic forces, which is obviously overevaluated in the modulus. A P.P.T. calculation in infinite field, while carefully replacing the shock in its experimental position ($\delta_m = 1^0$), provides very similar results to those of the guided airflow calculation. We can thus state that if the wall effects are not negligible, since the control surface has to be turned by 1.25° to have the same shock position, the effect on the unsteady coefficients (at this frequency) is mainly related to the displacements of the shock wave and not to the wave reflections on the wind tunnel walls.

/335

Airfoil RA 16 SC 1

Tests		δ_m	C_{z_δ}	φ^0	C_{m_δ}	φ^0
P.P.T.	a Veine guidée	0,5	2,31	— 41,3	0,77	— 6,2
		2,25	3,97	— 51,4	1,26	— 10,3
P.P.T.	b Champ infini	1°	3,57	— 31,8	1,19	— 4,4
Doublet		—	3,37	— 22,7	1,02	5,7

TABLE II
a-guided airflow, b-infinite field
Comparison of tests and calculations for the unsteady lift and moment

Table II also shows the calculation values by the Doublet-Lattice-Method. If the phase differences in figure 18 are more than 100° in some places, they become substantiallybreduced after integration; on the other hand, the modules are of the same order as those obtained by the small transonic perturbations calculation. This is relatively

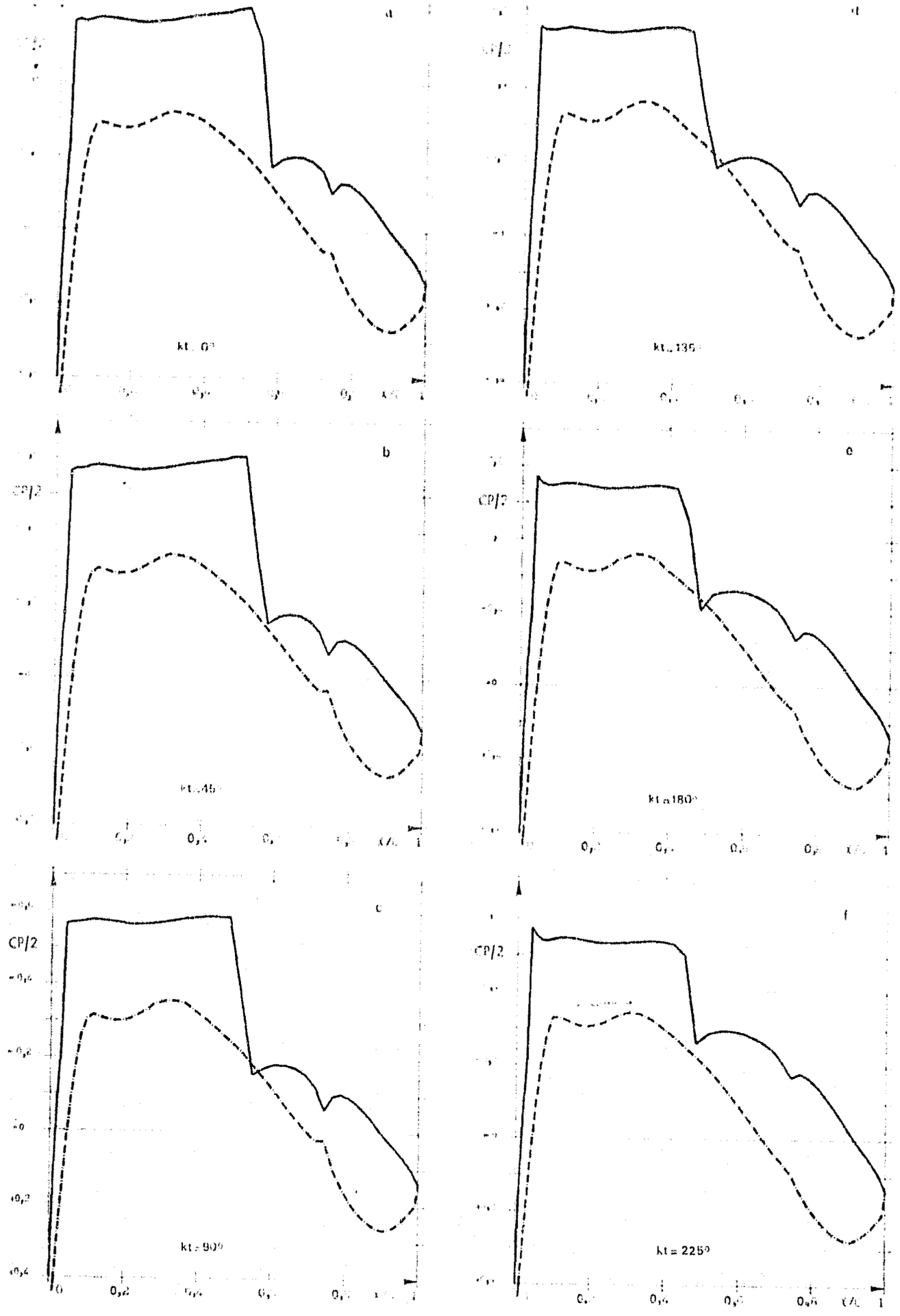

surprising, since the Doublet-Lattice-Method corresponds to a calculation of a flat plate wihtout angle (and of course, without shock).

It may be noted that the calculation - experiment comparisons have been made only for control surface effects, and the calculation of fluctuations also involve surging and pitching motions. From the point of view of the P.P.T. calculation, these motions do not present any special problems, but they would be less sensitive to viscous effects. In the examples considered here, the control surface is in fact heavily loaded, which facilitates separations, whereas on the rest of the airfoil, the viscous effects are more limited. The experimental and theoretical study of these two overall airfoil motions could make it possible to evaluate to what extent the use of a supercritical airfoil improves or damages the characteristics of a wing fluctuation.

VI.- CONCLUSIONS

In the research for an effective tool to solve the unsteady nad /339
two-dimensional transonic flows, the approximation of small perturbations is of interest. In fact, it allows a rather effective numerical solution based on an alternating direction implicit scheme. The initial limitations have been partially removed by establishing a functional approximation which relates the pressure coefficient to the equation of continuity and the boundary conditions, as well as by easing part of the constraints on the reduced frequency, without hindering the efficiency of the numerical solution.

Comparisons in the linear domain, in the presence of shock waves, with more sophisticated methods of calculation, such as the Euler type, are very encouraging. The calculations times are, in fact, up to 100 times faster, whereas the results coincide relatively well.

Comparison with wind tunnel tests, if it is more difficult, calls for a few remarks. It appears that the phase of the occurances is rather sensitive to the steady pressure field (and especially to the

position of the shock waves, whereas the modulus of unsteady aerodyanmic forces depends on viscous effects (with an equivalent steady pressure field). Accordingly, it seems necessary to take these last effects into account by preventing the viscous calculation from burdoning the coupling calculation. It is in fact desirable to take the boundary layer effects into account, and it is equally important to move to a three-dimensional calculation, the calculation times of which must remain reasonable.

This paper was submitted on July 23, 1979.

REFERENCES

1. Magnus R. and Yoshihara H., "Calculations of transonic flow over an oscillating airfoil", - AIAA Paper 75 - 98, Jan. 1975.

2. Magnus R. and Yoshihara H., "Calculation of the transonic oscillating flap with 'viscous' displacement effects", - AIAA Paper 76-327, July 1976.

3. Lerat A. and Sides J. "Numerical calculation of unsteady transonic flows", AGARD -CP-226, April 1977.

4. Lerat A. and Sides J., "Numerical simulation of unsteady transonic flows using the Euler equations in integral form", 1'Aviation et 1'Astronautique, Tel Aviv and Haifa (Israel), February 28 - March 1979.

5. Beam R. M. and Warming R.F., "An implicit finite difference algorithm for hyperbolic systems in conservation-law-form", J. Comput. Phys. 22, 1976, p. 87-110.

6. Steger J. L. "Implicit finite-difference simulation of flow about arbitrary two-dimensional geometries", AIAA Journal 16, 1978, p. 679-686.

7. Ballhaus W.F. and Steger J.L. "Implicit-approximate-factorization schemes for the low-frequency transonic equation", NASA TM-X-73.082, November 1975.

8. Ballhaus W.F. and Goorijan P.M., "Implicit finite-difference computations of unsteady transonic flows about airfoils", AIAA Journal, 15, 12, 1977 or AIAA Paper 77-205, January 1977.

9. Doublas J. and Gunn J., "Numer. Math. 6", 1964, p. 428.

10. Ballhaus W.F., "Some recent progress in transonic flow computation", VKI Lecture Series, Computational Fluid Dynamics, Von Karman Institute for Fluid Dynamics, Rhode-St-Genèse, Belgium, March 1976.

11. Krupp J.A. "The numerical calculation of plane steady transonic flows past thin lifting airfoils", Boeing Scientific Research Laboratory Report D180-12958-1, June 1971.

12. Van der Vooren J., Sloof J.W., Huizing G.H. and Van Essen A., "Remarks on the suitability of various transonic small perturbations equations to describe three-dimensional transonic flow", Symposium Transsonicum II Göttingen, September 8-13, 1975, Springer-Verlag.

13. Bateman H., "Notes on a differential equation which occurs in the two-dimensional motion of a compressible fluid and the associated variational problem", Proc. Roy. Series A. 125, 1929, p. 598-618.

14. Miles J.W., "The potential theory of unsteady supersonic flows", Cambridge University Press, 1959.

15. Couston M. and Angelini J.J., "Solution of nonsteady two-dimensional transonic small disturbances potential flow equation", Communication présenté au Symposium sur la Dynamique des Fluides, Instationnaires, organisée par l'ASME, San Francisco, December 10-15, 1978.

16. Murman E.M., "Analysis of embedded shock waves calculated by relaxation methods", Proceedings of AIAA Conference on Comp. Fluid Dynamics, Palm Springs, July 1973, p. 27-40.

17. Albano E. and Rodeen W.P., "A Doublet Lattice Method for calculating lift distributions on oscillating surfaces in subsonic flows", AIAA Paper 68-73, January 1968.

18. Magnus R. and Yoshihara H., "The transonic oscillating flap. A comparison of calculations with experiments", AGARD-CP-226, April 1977.

19. Magnus R., "Calculations of some unsteady transonic flows about the NACA 64A006 airfoils", AFFFL-TR-77-46, July 1977.

20. Tijdeman H., "Investigation of the transonic flow around oscillating airfoils", NLR Thesis, December 1977.

21. Ballhaus W.F., "Efficient solution of unsteady transonic flows about airfoils", AGARD-CP-226, April 1977.

22. Ehlers E., "A finite difference method for the solution of the transonic flow around harmonically oscillating wings", NASA CR-2257, 1974.

23. Grenon R. and Thers J. "Study of a supercritical airfoil with oscillating control surface in the subsonic and transonic flow", AGARD-CP-227, September 1977 or T.P. ONERA no. L977-136.

24. Grenon R. and Thers J. "Study of a supercritical airfoil with oscillating control surface in the subsonic and transonic flow"; 14th Colloque dAérodynamique Appliquée, Toulouse, 7-9 novembre 1977.

25. Grenon R., Desopper A. and Sides J., "Unsteady effects of a control surface in the subsonic and transonic two-dimensional flow", AGARD-CP-262, mai 1979.